"ML and MAP phase noise estimators for optical fiber FBMC-OQAM systems"

Rottenberg, François ; Nguyen, Trung-Hien ; Gorza, Simon-Pierre ; Horlin, François ; Louveaux, Jérôme

Abstract

This paper addresses the carrier phase recovery problem in Offset-QAM-based filterbank multicarrier (FBMC-OQAM) systems. The combined phase noise coming from the transmit and receive lasers, is known to induce a phase rotation of the demodulated symbols at the receiver. Several approaches have been proposed to recover the phase in FBMC-OQAM communication systems on optical fiber. Most of them have a significant complexity and do not make use of all information at disposal. In this paper, we propose two new estimators, obtained by minimizing a maximum likelihood (ML) and a maximum a posteriori (MAP) criteria. They use an error model formulation which allows to easily use priors on the phase noise statistics. By linearization of the error, an analytical solution is found for the phase error, which avoids the need for multiple phase tests. Simulation results demonstrate the better performance of the proposed estimators with respect to state of the art solutions in the low signal-to-nois...

Document type : *Communication à un colloque (Conference Paper)*

ML and MAP Phase Noise Estimators for Optical Fiber FBMC-OQAM Systems

François Rottenberg*†, Trung-Hien Nguyen†, Simon-Pierre Gorza†, François Horlin† and Jérôme Louveaux*
*ICTEAM institute, Université catholique de Louvain, Belgium
† OPERA department, Université libre de Bruxelles, Belgium

***Abstract*—This paper addresses the carrier phase recovery problem in Offset-QAM-based filterbank multicarrier (FBMC-OQAM) systems. The combined phase noise coming from the transmit and receive lasers, is known to induce a phase rotation of the demodulated symbols at the receiver. Several approaches have been proposed to recover the phase in FBMC-OQAM communication systems on optical fiber. Most of them have a significant complexity and do not make use of all information at disposal. In this paper, we propose two new estimators, obtained by minimizing a maximum likelihood (ML) and a maximum *a posteriori* (MAP) criteria. They use an error model formulation which allows to easily use priors on the phase noise statistics. By linearization of the error, an analytical solution is found for the phase error, which avoids the need for multiple phase tests. Simulation results demonstrate the better performance of the proposed estimators with respect to state of the art solutions in the low signal-to-noise (SNR) regime and for a small number of subcarriers.**

***Keywords*—Filter-bank multicarrier, offset QAM, coherent detection, carrier phase estimation**

I. Introduction

Offset-QAM-based filterbank multicarrier (FBMC-OQAM) has been recently proposed in optical fiber communication systems [1]–[5]. FBMC-OQAM modulations use a pulse shape which is well localized in time and frequency, making the system more robust against time and frequency variations of the channel [6]. One of the main advantages of FBMC-OQAM for optical fiber communication is its increased spectral efficiency. Indeed, thanks to the very low spectral leakage of its prototype filter, it is sufficient to insert a very small guard band between unsynchronized optical laser, which results in a higher spectral efficiency [5].

Thanks to the recent advents in electronic circuits, digital signal processing (DSP) is becoming more prevalent in modern optical coherent systems. The laser phase noise is one of the crucial impairments in such systems. The phase noise induces a rotation of the signal after the demodulation process at the receiver. Carrier phase recovery (CPR) becomes an essential DSP block in order to recover the transmitted signals. Different CPR algorithms have already been proposed. Because of the particular structure of the intrinsic interference inherent to OQAM modulations, the extension to OQAM systems is not straightforward. The work of [1] proposed a modified blind phase search (M-BPS) algorithm which takes advantage of the OQAM modulation to track the phase variations of the laser. The M-BPS algorithm tries to find the optimal phase estimate by performing a certain number of phase trials. The final phase estimate is given at each multicarrier symbol by the phase trial that minimizes a certain cost function. The approach has a significant complexity of implementation, even though a simplified version has been proposed in [2] with negligible performance loss. Moreover, in practice, only a finite number of phase trials can be tested, which induces a discretization error.

In this paper, we propose two new estimators for the laser phase noise in optical FBMC/OQAM systems, namely, a maximum likelihood (ML) estimator and a maximum *a posteriori* (MAP) estimator. The novelty of the approach is plural. Since the phase is assumed to change slowly over time, the measurement model is formulated as a function of the phase error with respect to the previous phase estimate. This allows to easily exploit the known *a priori* statistics of the phase noise. By linearization of the system model, closed-form expressions are found that avoid the need of multiple phase tests. This decreases the complexity of the algorithm and at the same time suppresses the discretization error due to the limited number of phase tests of the M-BPS algorithm. Furthermore, a part of the intrinsic interference is estimated based on previous and current decoded symbols. The ML and MAP estimates are obtained by combining the outputs of all subcarriers, which makes the system more robust to additive noise effect. Moreover, the ML and MAP estimators do not suffer from phase ambiguity problems as opposed to the M-BPS algorithm. The performance of the proposed estimators is demonstrated by simulations. It is shown that the proposed algorithms outperform the state of the art M-BPS algorithm in the low signal-to-noise ratio (SNR) region and when a small number of subcarriers used.

A. Notations

Vectors and matrices are denoted by bold lowercase and uppercase letters, respectively. Superscripts * and ^{T} stand for conjugate and transpose operators. The symbols $\mathbb{E}$, $|.|$, $\Im$ and $\Re$ denote the expectation, the determinant of a matrix, imaginary and real parts, respectively. The notation a^R and a^I is an alternative notation for the real and imaginary parts of a respectively. $\jmath$ is the imaginary unit. $\mathbf{I}_N$ denotes the identity matrix of size $N \times N$. $\otimes$ stands for the Kronecker product.

II. System model

We consider an FBMC-OQAM system with $2M$ subcarriers. The real-valued transmitted symbols, denoted by $d_{m,l}$, are FBMC-OQAM modulated using a prototype pulse $g[n]$ of length $L_g = 2\kappa M$ where κ is the overlapping factor and with

unit energy. The transmitted signal $s[n] \in \mathbb{C}$ can be written as

$$s[n] = \sum_{l=-\infty}^{+\infty} \sum_{m=0}^{2M-1} d_{m,l} g_{m,l}[n]$$

where $g_{m,l}[n] = \theta_{m,l} g[n - lM] e^{\jmath \frac{2\pi}{2M} m(n - lM - \frac{L_g - 1}{2})}$ with $\theta_{m,l} = \jmath^{l+m}$. To focus on the phase noise impact, we consider only one polarization mode and we assume that the chromatic dispersion is perfectly compensated at the receiver. The received signal, denoted by $r[n]$, is only impacted by phase noise and additive noise,

$$r[n] = s[n] e^{\jmath \phi[n]} + w[n].$$

The phase noise is modeled as a Wiener process, i.e., $\phi[n + 1] = \phi[n] + \nu[n]$ where $\nu[n]$ is an independent real Gaussian random variable with zero mean and variance $\sigma_\nu^2 = 2\pi \Delta\nu \frac{T}{2M}$ [8]. The parameter $\Delta\nu$ refers to the combined laser linewidth. The noise samples $w[n]$ are additive circularly-symmetric white Gaussian noise samples with zero mean and variance N_0, i.e., $w[n] \sim \mathcal{CN}(0, N_0)$. At the receiver, the signal after demodulation, at subcarrier m_0 and multicarrier symbol l_0, denoted by z_{m_0,l_0}, may be written as

$$\begin{aligned} z_{m_0,l_0} &= \sum_{n=0}^{L_g-1} r[n] g^*_{m_0,l_0}[n] \\ &= \sum_{l,m} d_{m,l} \sum_{n=0}^{L_g-1} g_{m,l}[n] g^*_{m_0,l_0}[n] e^{\jmath \phi[n]} + w_{m_0,l_0} \end{aligned}$$

where w_{m_0,l_0} is the filtered noise. Furthermore, we assume that the phase noise is slowly varying with respect to the symbol duration. Hence, the phase noise can be viewed as constant during one multicarrier symbol transmission,

$$z_{m_0,l_0} \approx d_{m_0,l_0} e^{\jmath \phi_{l_0}} + \jmath u_{m_0,l_0} e^{\jmath \phi_{l_0}} + w_{m_0,l_0}$$

where $\jmath u_{m_0,l_0} = \sum_{(m,l) \neq (m_0,l_0)} d_{m,l} t_{m,m_0,l,l_0}$ with $t_{m,m_0,l,l_0} = \sum_{n=0}^{L_g-1} g_{m,l}[n] g^*_{m_0,l_0}[n]$. The symbol $\jmath u_{m_0,l_0}$ is purely imaginary and is commonly referred to as intrinsic interference. The equalization is performed by simply applying a phase correction and real conversion, i.e., $\hat{d}_{m_0,l_0} = \Re\{z_{m_0,l_0} e^{-\jmath \hat{\phi}_{l_0}}\}$ where $\hat{\phi}_{l_0}$ is the estimate of the phase noise at multicarrier symbol l_0. Accurate estimation of the phase noise is of crucial importance to avoid leakage of the intrinsic interference on the symbol of interest.

III. ML AND MAP PHASE ESTIMATORS

Let us assume that an initial phase estimate can be obtained at the beginning of the transmission. After this initialization phase, the modem switches in tracking mode and does not use pilot symbols. Let us denote the estimate of the previous phase at multicarrier symbol $l - 1$ by $\hat{\phi}_{l-1}$. We want an estimate of the current phase ϕ_l that we denote by $\hat{\phi}_l$.

Since the phase noise is assumed to be slowly varying over the symbol duration, we propose to estimate the phase error, defined as $\epsilon_l = \phi_l - \hat{\phi}_{l-1}$ and its estimate, $\hat{\epsilon}_l = \hat{\phi}_l - \hat{\phi}_{l-1}$, instead of re-estimating ϕ_l from scratch as in [1], [2]. At first, we perform a rotation of angle $-\hat{\phi}_{l-1}$ on $z_{m,l}$,

$$\begin{aligned} \tilde{z}_{m,l} &= e^{-\jmath \hat{\phi}_{l-1}} z_{m,l} \\ &= d_{m,l} e^{\jmath \epsilon_l} + \jmath u_{m,l} e^{\jmath \epsilon_l} + \tilde{w}_{m,l}. \end{aligned}$$

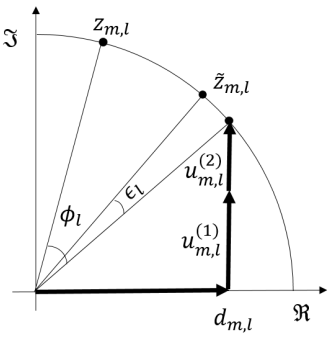

Fig. 1. Illustration of the signal model on the complex plane without additive noise.

Since the phase noise is assumed to vary slowly, a first estimation of the symbols $d_{m,l}$ at multicarrier symbol l can be obtained by taking the real part of $\tilde{z}_{m,l}$ and performing a direct decision. Moreover, thanks to the current and previously decoded symbols, a part of the intrinsic interference can be estimated. We re-write $u_{m,l}$ as

$$\begin{aligned} u_{m_0,l_0} &= u^{(1)}_{m_0,l_0} + u^{(2)}_{m_0,l_0} \\ u^{(i)}_{m_0,l_0} &= \sum_{(m,l) \in \Omega^{(i)}_{m_0,l_0}} d_{m,l} \Im\{t_{m,m_0,l,l_0}\}, \quad i = 1, 2 \end{aligned}$$

where $u^{(1)}_{m,l}$ corresponds to the intrinsic interference due to previous and current decoded symbols which can be estimated based on decisions, i.e., $\Omega^{(1)}_{m_0,l_0}$ is the set of indices (m, l) such that $m \in \{0, ..., 2M - 1\}, l \leq l_0$ and $u^{(2)}_{m,l}$ is the intrinsic interference due to future symbols, i.e., $\Omega^{(2)}_{m_0,l_0}$ is the set of indices (m, l) such that $m \in \{0, ..., 2M - 1\}, l > l_0$. Fig. 1 illustrates the signal model under consideration with no additive noise ($w_{m_0,l_0} = 0$). Of course, the knowledge of $u^{(1)}_{m,l}$ can help to improve the performance but also increases the complexity of the algorithm due to the necessary computation of $u^{(1)}_{m,l}$. In practice, if the prototype pulse is well localized in time and frequency, the set $\Omega^{(1)}_{m_0,l_0}$ can be restricted to the close neighbors of (m_0, l_0) and the complexity might be decreased by considering less neighboring symbols in the estimation of $u^{(1)}_{m,l}$. The complexity-performance trade-off will be further discussed in Section IV. Note that the symbol $d_{m,l} + \jmath u^{(1)}_{m,l}$ can be seen as a kind of pseudo-pilot symbol [9]. However, it includes only one part of the intrinsic interference and it is based on direct decisions and not pilots.

Since the phase noise at instant l does not depend on the subcarrier index, it makes sense to combine all subcarriers to jointly estimate this phase factor. Moreover, the use of all subcarriers makes the estimator more robust against the noise effect. In the following sections, the outputs of all subcarriers will be considered.

A. ML estimator

The ML estimator of ϵ_l is the one that maximizes the likelihood of the demodulated symbols given ϵ_l, based on

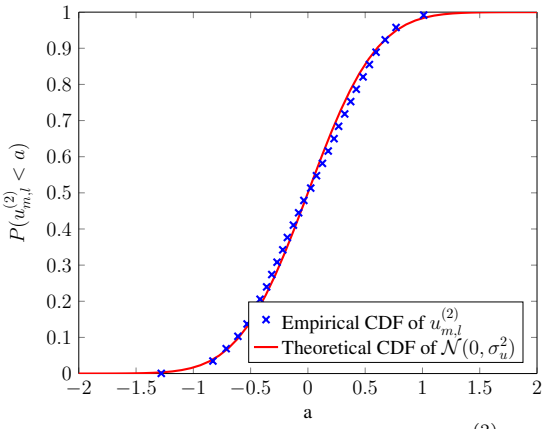

Fig. 2. Empirical cumulative density function (CDF) of $u_{m,l}^{(2)}$ versus CDF of a zero mean Gaussian random variable with variance σ_u^2.

current available decisions,

$$\hat{\epsilon}_l^{\text{ML}} = \arg\max_{\epsilon_l} f(\tilde{z}_{0,l}, ..., \tilde{z}_{2M-1,l}|\epsilon_l).$$

Since one part of the intrinsic interference, $u_{0,l}^{(2)}, ..., u_{2M-1,l}^{(2)}$, cannot be estimated, we will consider it as noise. The distribution of $u_{m,l}^{(2)}$ is an intricate combination of the real transmitted symbols. To simplify the design, we will assume that $u_{m,l}^{(2)}$ is normally distributed with zero mean and variance σ_u^2, i.e., $u_{m,l}^{(2)} \sim \mathcal{N}(0, \sigma_u^2)$. Assuming that the transmitted symbols $d_{m,l}$ are independent and of variance $E_s/2$, the variance σ_u^2 is given by

$$\sigma_u^2 = \frac{E_s}{2} \sum_{(m,l)\in\Omega_{m_0,l_0}^{(2)}} \Im^2\left\{t_{m,m_0,l,l_0}\right\}.$$

Note that depending on the number of neighboring symbols included in the set $\Omega_{m_0,l_0}^{(2)}$, the value of σ_u^2 might change. In the limit case where $\Omega_{m_0,l_0}^{(1)} = \emptyset$, there is no estimation of the intrinsic interference, i.e., $u_1 = 0$. Fig. 2 plots the empirical distribution of $u_{m,l}^{(2)}$ compared to the distribution of a Gaussian random variable with variance σ_u^2. This justifies the assumption of approximating the distribution $u_{m,l}^{(2)}$ as Gaussian. One should remember that $u_{m,l}^{(2)}$ is purely real. Hence, the noise statistics are not circularly symmetric. To take this into account, we rewrite the measurement model at all subcarriers in an extended all-real form as

$$\mathbf{z} = \mathbf{C}\boldsymbol{\theta} + \mathbf{w}$$

where we defined $\mathbf{z} = \left(\tilde{z}_{0,l}^R, \tilde{z}_{0,l}^I, \ldots, \tilde{z}_{2M-1,l}^R, \tilde{z}_{2M-1,l}^I\right)^T$, $\mathbf{C} = \left(\mathbf{C}_{0,l}^T, \ldots, \mathbf{C}_{2M-1,l}^T\right)^T$, $\theta = (\cos(\epsilon_l), \sin(\epsilon_l))^T$, $\mathbf{w} = \left(\tilde{\mathbf{w}}_{0,l}^T, \ldots, \tilde{\mathbf{w}}_{2M-1,l}^T\right)^T$ and

$$\mathbf{C}_{m,l} = \begin{pmatrix} d_{m,l} & -u_{m,l}^{(1)} \\ u_{m,l}^{(1)} & d_{m,l} \end{pmatrix}, \tilde{\mathbf{w}}_{m,l} = \begin{pmatrix} -u_{m,l}^{(2)}\sin(\epsilon_l) + \tilde{w}_{m,l}^R \\ u_{m,l}^{(2)}\cos(\epsilon_l) + \tilde{w}_{m,l}^I \end{pmatrix}.$$

One can verify that, under previous assumptions, the vector of real noise samples $\mathbf{w}$ is normally distributed with zero mean and a covariance matrix $\mathbf{R}_w$ that depends on ϵ_l. In FBMC-OQAM systems, the prototype pulse, modulated around a specific time-frequency bin (m, l), overlaps with neighboring subcarriers and multicarrier symbols. This implies correlation of the additive noise and the intrinsic interference, i.e., $\mathbf{R}_w$ is not diagonal. Taking into account this interference could help to average the noise effect. However, this would significantly increase the complexity of the design. Therefore, we here choose to neglect inter-carrier correlation. Matrix $\mathbf{R}_w$ then becomes block diagonal, i.e., $\mathbf{R}_w = \mathbf{I}_{2M} \otimes \mathbf{R}_m$, with $\mathbf{R}_m$ given by

$$\mathbf{R}_m = \begin{pmatrix} \frac{N_0}{2} + \sigma_u^2\sin^2(\epsilon_l) & -\sigma_u^2\sin(\epsilon_l)\cos(\epsilon_l) \\ -\sigma_u^2\sin(\epsilon_l)\cos(\epsilon_l) & \frac{N_0}{2} + \sigma_u^2\cos^2(\epsilon_l) \end{pmatrix}.$$

We are now in the position to write the expression of the likelihood $f(\mathbf{z}|\epsilon_l) = f(\tilde{z}_{0,l}, ..., \tilde{z}_{2M-1,l}|\epsilon_l)$,

$$f(\mathbf{z}|\epsilon_l) = \frac{1}{\sqrt{(2\pi)^{4M}|\mathbf{R}_w|}} e^{-\frac{1}{2}(\mathbf{z}-\mathbf{C}\boldsymbol{\theta})^T\mathbf{R}_w^{-1}(\mathbf{z}-\mathbf{C}\boldsymbol{\theta})}.$$

Noting that $|\mathbf{R}_w| = (\frac{N_0}{2}(\frac{N_0}{2} + \sigma_u^2))^{2M}$ which does not depend on ϵ_l and that $\mathbf{R}_w^{-1} = \mathbf{I}_{2M} \otimes \mathbf{R}_m^{-1}$ is block diagonal with

$$\mathbf{R}_m^{-1} = \frac{\begin{pmatrix} \frac{N_0}{2} + \sigma_u^2\cos^2(\epsilon_l) & \sigma_u^2\sin(\epsilon_l)\cos(\epsilon_l) \\ \sigma_u^2\sin(\epsilon_l)\cos(\epsilon_l) & \frac{N_0}{2} + \sigma_u^2\sin^2(\epsilon_l) \end{pmatrix}}{\frac{N_0}{2}(\frac{N_0}{2} + \sigma_u^2)},$$

the maximum likelihood estimator is given by

$$\begin{aligned}\hat{\epsilon}_l^{\text{ML}} &= \arg\max_{\epsilon_l} \log f(\tilde{\mathbf{z}}|\epsilon_l) \\ &= \arg\max_{\epsilon_l} -\frac{1}{2}(\mathbf{z}-\mathbf{C}\boldsymbol{\theta})^T\mathbf{R}_w^{-1}(\mathbf{z}-\mathbf{C}\boldsymbol{\theta})\end{aligned}$$

where we removed the constant term of the log-likelihood that does not depend on ϵ_l. After several mathematical manipulations and keeping only the terms that depend on ϵ_l, the expression simplifies to

$$\begin{aligned}\hat{\epsilon}_l^{\text{ML}} &= \arg\max_{\epsilon_l} L_1 \\ L_1 &= -\frac{\sigma_u^2}{2}\sum_{m=0}^{2M-1} \Re\{\tilde{z}_{m,l}e^{-\jmath\epsilon_l}\}\left(\Re\{\tilde{z}_{m,l}e^{-\jmath\epsilon_l}\} - 2d_{m,l}\right) \\ &\quad + \frac{N_0}{2}\sum_{m=0}^{2M-1} \Re\left\{\tilde{z}_{m,l}\left(d_{m,l} - \jmath u_{m,l}^{(1)}\right)e^{-\jmath\epsilon_l}\right\}.\end{aligned}$$

The two terms in the above expression have an intuitive meaning. The maximization of the first term, proportional to $-\sigma_u^2$ tends to find the rotation ϵ_l such that, after taking the real part, the contribution due to remaining intrinsic interference disappears and the symbol $d_{m,l}$ is recovered, i.e., $\Re\{\tilde{z}_{m,l}e^{-\jmath\epsilon_l}\} = d_{m,l}$. The maximization of the second term aims at finding the value of ϵ_l that aligns the observations $\tilde{z}_{m,l}$ with the "partial" pseudo-pilots $d_{m,l} + \jmath u_{m,l}^{(1)}$, especially when the additive noise power N_0 is large. This problem is not trivial to optimize due to the non polynomial dependence in ϵ_l. One idea would be to test different phase trials, evaluate the likelihood and keep the best test, as it was done in [1], [2] but using a different metric. However, this would significantly increase the complexity of the algorithm. Moreover, the fact that in practice, only a finite number of phase trials can be tested induces a discretization error.

In order to reduce the complexity, we derive a closed-form solution. Due to the fact that ϵ_l is close to zero, the term $e^{-\jmath\epsilon_l}$

can be well approximated by the first order Taylor expansion given by $e^{-\jmath\epsilon_l} \approx 1-\jmath\epsilon_l$. Note that this assumption makes sense due to the slowly varying nature of the phase noise. We will further show, through simulations, that the error induced by this linearization is negligible and does not impact the system performance. This leads to

$$\begin{aligned}\hat{\epsilon}_l^{\mathrm{ML}} \approx \arg\max_{\epsilon_l} & -\frac{\sigma_u^2}{2}\sum_{m=0}^{2M-1}\left(\Re\{\tilde{z}_{m,l}(1-\jmath\epsilon_l)\}\right)^2 \\ & + \sigma_u^2\sum_{m=0}^{2M-1}\left(\Re\{\tilde{z}_{m,l}(1-\jmath\epsilon_l)\}\right)d_{m,l} \\ & + \frac{N_0}{2}\sum_{m=0}^{2M-1}\Re\left\{\tilde{z}_{m,l}\left(d_{m,l}-\jmath u_{m,l}^{(1)}\right)(1-\jmath\epsilon_l)\right\},\end{aligned}$$

which is a quadratic expression in ϵ_l. We finally obtain

$$\hat{\epsilon}_l^{\mathrm{ML}} \approx \frac{\sum_m(\tilde{z}_{m,l}^I(\frac{N_0}{2}+\sigma_u^2)d_{m,l} - \tilde{z}_{m,l}^R\frac{N_0}{2}u_{m,l}^{(1)} - \sigma_u^2\tilde{z}_{m,l}^R\tilde{z}_{m,l}^I)}{\sigma_u^2\sum_m(\tilde{z}_{m,l}^I)^2}.$$

Hence, the current phase can be estimated as $\hat{\phi}_l = \hat{\phi}_{l-1} + \hat{\epsilon}_l^{\mathrm{ML}}$ and the symbols $d_{m,l}$ can be re-estimated using this update of the phase.

B. MAP estimator

The ML estimator does not use the *a priori* distribution of ϵ_l. In practice, the transmit and receive lasers are known. Hence the linewidth can be estimated and we can use this knowledge to improve the estimation. The MAP estimator of ϵ_l is given by

$$\hat{\epsilon}_l^{\mathrm{MAP}} = \arg\max_{\epsilon_l} f(\mathbf{z}|\epsilon_l)f(\epsilon_l). \tag{1}$$

Assuming that the previous phase estimate is close to the actual phase, we can approximate $\epsilon_l = \phi_l - \hat{\phi}_{l-1}$ by $\epsilon_l \approx \phi_l - \phi_{l-1}$. Under this assumption, ϵ_l is normally distributed with zero mean and variance $\sigma_\epsilon^2 = M\sigma_\nu^2 = \pi\Delta\nu T$, i.e.,

$$f(\epsilon_l) = \frac{1}{\sqrt{2\pi\sigma_\epsilon^2}}e^{-\frac{\epsilon_l^2}{2\sigma_\epsilon^2}}, \quad \log f(\epsilon_l) = D - \frac{\epsilon_l^2}{2\sigma_\epsilon^2},$$

where D is a constant that does not depend on ϵ_l. Taking the logarithm of the expression in (1), the MAP estimator of ϵ_l is the solution of

$$\begin{aligned}\hat{\epsilon}_l^{\mathrm{MAP}} &= \arg\max_{\epsilon_l} L_2 \\ L_2 &= -\frac{\sigma_u^2}{2}\sum_{m=0}^{2M-1}\Re\{\tilde{z}_{m,l}e^{-\jmath\epsilon_l}\}\left(\Re\{\tilde{z}_{m,l}e^{-\jmath\epsilon_l}\} - 2d_{m,l}\right) \\ &\quad + \frac{N_0}{2}\sum_{m=0}^{2M-1}\Re\left\{\tilde{z}_{m,l}\left(d_{m,l}-\jmath u_{m,l}^{(1)}\right)e^{-\jmath\epsilon_l}\right\} - \frac{\epsilon_l^2}{2}\sigma_{\mathrm{MAP}}^2.\end{aligned}$$

where $\sigma_{\mathrm{MAP}}^2 = \frac{\frac{N_0}{2}(\frac{N_0}{2}+\sigma_u^2)}{\sigma_\epsilon^2}$. If, as in the derivations of the ML estimator, we use the first order approximation of $e^{-\jmath\epsilon_l}$, we obtain

$$\hat{\epsilon}_l^{\mathrm{MAP}} \approx \frac{\sum_m(\tilde{z}_{m,l}^I(\frac{N_0}{2}+\sigma_u^2)d_{m,l} - \tilde{z}_{m,l}^R\frac{N_0}{2}u_{m,l}^{(1)} - \sigma_u^2\tilde{z}_{m,l}^R\tilde{z}_{m,l}^I)}{\sigma_u^2\sum_m(\tilde{z}_{m,l}^I)^2 + \sigma_{\mathrm{MAP}}^2}.$$

One can see that the MAP estimator expression is very close to the ML estimator. Intuitively, the parameter σ_{MAP}^2 adjusts the estimation depending on the linewidth of the laser. If the linewidth is small, σ_ϵ^2 will be low as well and σ_{MAP}^2 will be high, which will decrease in the end the value of the estimate. This makes sense since we have the *a priori* knowledge that ϵ_l is low and we should then penalize large values of ϵ_l. Finally, the current phase noise is estimated as $\hat{\phi}_l = \hat{\phi}_{l-1} + \hat{\epsilon}_l^{\mathrm{MAP}}$ and the symbols $d_{m,l}$ are re-estimated using this update of the phase. Note that, the ML and MAP estimators do not suffer from ambiguity problem [10] as could be the case for the M-BPS algorithm, which can recover the phase only up to a multiple of π.

Note that in the case where no part of the intrinsic interference is estimated, the MAP estimator simplifies to

$$\hat{\epsilon}_{l,u^{(1)}=0}^{\mathrm{MAP}} \approx \frac{(\frac{N_0}{2}+\sigma_u^2)\sum_m\tilde{z}_{m,l}^I d_{m,l} - \sigma_u^2\sum_m\tilde{z}_{m,l}^R\tilde{z}_{m,l}^I}{\sigma_u^2\sum_m(\tilde{z}_{m,l}^I)^2 + \sigma_{\mathrm{MAP}}^2},$$

where σ_u^2 should be re-computed based on the new neighborhood defined by $\Omega_{m_0,l_0}^{(2)}$. One can see that the estimator $\hat{\epsilon}_{l,u^{(1)}=0}^{\mathrm{MAP}}$ has a very low complexity of implementation.

IV. Simulation results

This sections aims at validating the performance of the proposed estimators through simulations. We will assume a laser linewidth $\Delta\nu$ of 1 MHz and a bandwidth of 30 GHz, which corresponds to a sampling period $\frac{T}{2M}$ of 33 ps. Note that since the bandwidth is fixed, if we increase the number of subcarriers $2M$, the symbol period T is increased as well. As a consequence, the system becomes more sensitive to the laser phase noise since the phase has experienced a larger variation during one symbol duration. To take that into account, we define the normalized bandwidth as the product of the combined linewidth and symbol duration, i.e., $\Delta\nu T$. In the simulations, the theoretical curve of a system without phase noise is also plotted, as a benchmark. The prototype filter used in the simulations is the Phydyas filter [11] with overlapping factor set to four.

In Fig. 3, the symbol error rate (SER) is simulated for FBMC-OQAM systems using different implementations of the proposed estimators. A 4-OQAM and a 16-OQAM constellations are considered. The ML curve corresponds to the derived ML estimator denoted by $\hat{\epsilon}_l^{\mathrm{ML}}$, based on the linearization of $e^{-\jmath\epsilon_l}$ and where $u_{m,l}^{(1)}$ is estimated based on all current and previously decoded symbols. The MAP curve corresponds to the derived MAP estimator denoted by $\hat{\epsilon}_l^{\mathrm{MAP}}$ which is very similar to the ML estimator but includes the *a priori* distribution of the phase noise. As can be seen, the MAP estimator does not provide a high gain with respect to the ML estimator, except at very low SNR for the 4-OQAM constellation. Furthermore, the MAP curve with $u^{(1)} = 0$ corresponds to the MAP estimator with no estimation at all of the intrinsic interference, denoted by $\hat{\epsilon}_{l,u^{(1)}=0}^{\mathrm{MAP}}$. Note that this estimator is less complex and achieves the same performance as the the estimator $\hat{\epsilon}_l^{\mathrm{MAP}}$. Therefore, we conclude that estimating part of the intrinsic interference is not really useful and should be avoided to decrease the estimation complexity. In the following, we only consider the MAP estimator $\hat{\epsilon}_{l,u^{(1)}=0}^{\mathrm{MAP}}$ since it achieves the best trade-off between performance and complexity.

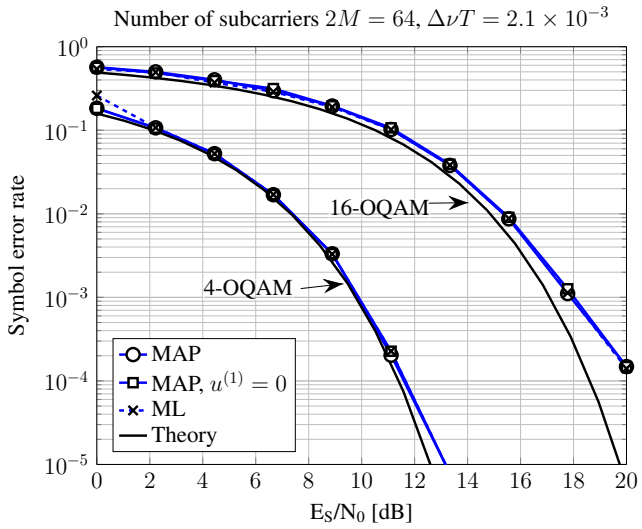

Fig. 3. Comparison of different proposed estimators.

TABLE I. COMPLEXITY OF THE ALGORITHMS IN TERMS OF REAL MULTIPLICATIONS AND DECISIONS. B IS THE NUMBER OF PHASE TESTS.

	Real multiplications	Decisions
M-BPS	$4MB$	$2MB$
MAP, $u^{(1)} = 0$	$18M + 4$	$4M$

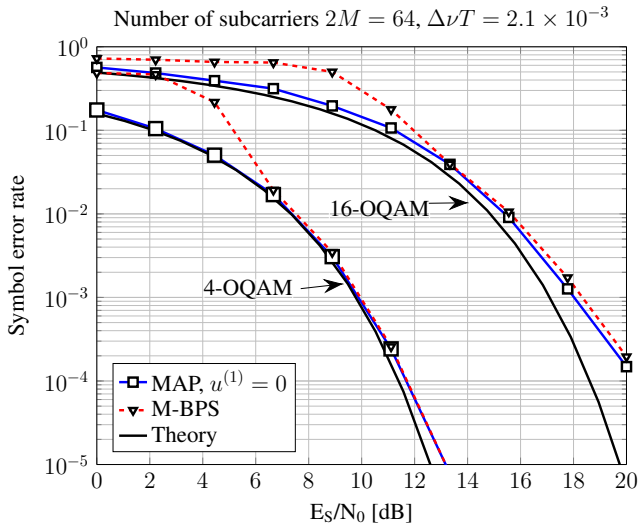

Fig. 4. Comparison of the proposed MAP estimator with the state of the art M-BPS algorithm as a function of the SNR.

In Fig. 4 and Fig. 5, the SER of an FBMC-OQAM system using the proposed MAP estimator $\hat{\epsilon}^{\text{MAP}}_{l,u^{(1)}=0}$ is compared to the state of the art M-BPS algorithm, as detailed in [2]. The M-BPS algorithm is here implemented with a number of phase tests B set to 20. The complexity of those two algorithms is compared in Table I. One can see that the proposed estimator uses about 4 times less real multiplications and 10 times less decisions than the M-BPS algorithm (for $B = 20$).

Fig. 4 compares the two methods as a function of the SNR. Again, two constellation sizes are considered, namely, a 4-OQAM and a 16-OQAM. The results show that M-BPS

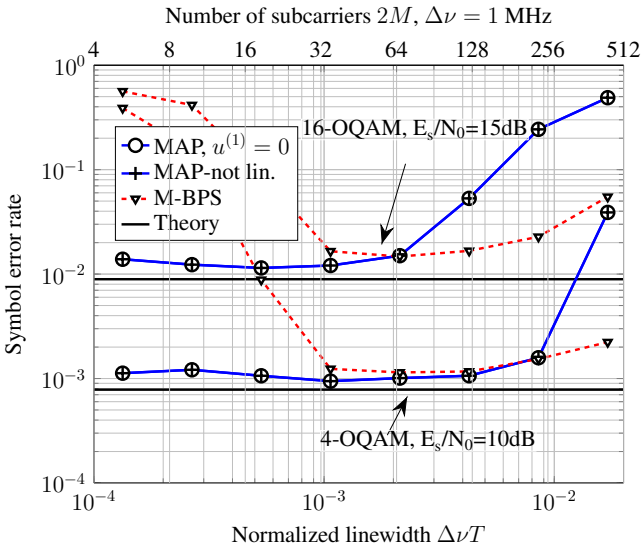

Fig. 5. Comparison of the proposed MAP estimator with the state of the art M-BPS algorithm as a function of the normalized linewidth.

performs significantly worse at low SNR level, especially for a higher constellation size. At medium and high SNR values, the performances of the two algorithms are equivalent. The worse performance of the M-BPS algorithm at low SNR can be explained by the M-BPS metric, which is obtained based on the assumption of a high SNR regime. On the other hand, the proposed MAP estimator does not make that assumption and performs well at low SNR. Furthermore, it does not suffer from the discretization error due the limited number of phase tests of the M-BPS algorithm. It can also use its *a priori* information on the phase error to improve the phase noise estimation. On top of that, the complexity of the MAP estimator is drastically reduced.

Fig. 5 compares the proposed MAP estimator and the M-BPS algorithm as a function of the normalized linewidth for fixed SNR values. For the 16-OQAM constellation, the SNR is fixed to $E_s/N_0 = 15$ dB while for the 4-OQAM constellation, the SNR is fixed to $E_s/N_0 = 10$ dB. To better understand the figure, one should remember that the transmission bandwidth is fixed and hence the ratio $\frac{T}{2M}$. This means that, if the normalized linewidth $\Delta\nu T = \Delta\nu \frac{T}{2M} 2M$ increases, the number of subcarriers $2M$ has increased as well, as indicated in the upper x axis of Fig. 5.

It can readily be seen in Fig. 5 that the M-BPS algorithm performs very poorly for low normalized linewidth. This comes from the fact that the number of subcarriers is low and the noise effect is not well averaged by the algorithm. As the normalized linewidth increases, and hence the number of subcarriers, the M-BPS starts to perform better. On the other hand, the MAP estimator performs well at low to moderate normalized linewidth since it does not make any assumption on the working SNR regime.

Furthermore, for high normalized linewidth values, the performance of the two algorithms begins to decrease. This comes from the fact that the basic assumption that the phase is constant during one multicarrier symbol transmission is not true anymore. One can see that the MAP estimator is more

sensitive and is outperformed for high normalized linewidth by the M-BPS algorithm. One could think that the degradation comes from the linearization error of the approximation $e^{-\jmath\epsilon_l} \approx 1 - \jmath\epsilon_l$. To show the impact of this error, we plotted a MAP curve with no linearization, which achieves exactly the same performance as the MAP estimator. This curve is obtained by computing the MAP criterion for a high number of phase tests and keeping the best phase test. Therefore, we explain the worse performance of the MAP algorithm by the fact that the algorithm first estimates the current real symbols by performing a direct decision using the estimate of the phase at the previous multicarrier symbol, which is not the case for the M-BPS algorithm. In other words, the algorithm is limited by the propagation of the decision errors. One could avoid it by changing our algorithm and considering the current multicarrier symbol as an unknown random variable too and try a different number of phase trials. For each phase test, we would perform a direct decision and compute the *a posteriori* probability and keep the best test, as in the M-BPS algorithm but using a different cost function. Of course, this would increase the complexity.

V. Conclusion

Two estimators have been proposed for carrier phase recovery in optical FBMC-OQAM systems. The first one was obtained by maximization of the likelihood of the demodulated signal while the second one was found by maximizing the *a posteriori* distribution of the received signal. For both estimators, a closed form expression was derived, based on a first order approximation of the signal model, which leads to a significant reduction of complexity with respect to state of the art solutions. The impact of estimating part of the intrinsic interference based on previous and current decoded symbols was studied. It was shown through simulations that it does not provide significant gain of performances. Simulation results have also shown that the proposed estimators outperform state of the art solution in the low SNR regime and for a small number of subcarriers.

Acknowledgment

The research reported herein was partly funded by Fonds pour la Formation à la Recherche dans l'Industrie et dans l'Agriculture (F.R.I.A.) and by the Belgian Fonds National de la Recherche Scientifique - FNRS (PDR T.1039.15).

References

[1] H. Tang, M. Xiang, S. Fu, M. Tang, P. Shum, and D. Liu, "Feed-forward carrier phase recovery for offset-QAM Nyquist WDM transmission," *Opt. Express*, vol. 23, no. 5, pp. 6215–6227, Mar. 2015. [Online]. Available: http://www.opticsexpress.org/abstract.cfm?URI=oe-23-5-6215

[2] T.-H. Nguyen, S.-P. Gorza, J. Louveaux, and F. Horlin, "Low-complexity blind phase search for filter bank multicarrier Offset-QAM optical fiber systems," in *Advanced Photonics 2016 (IPR, NOMA, Sensors, Networks, SPPCom, SOF)*. Optical Society of America, 2016, p. SpW2G.2. [Online]. Available: http://www.osapublishing.org/abstract.cfm?URI=SPPCom-2016-SpW2G.2

[3] J. Fickers, A. Ghazisaeidi, M. Salsi, G. Charlet, P. Emplit, and F. Horlin, "Multicarrier Offset-QAM for Long-Haul Coherent Optical Communications," *Journal of Lightwave Technology*, vol. 32, no. 24, pp. 4671–4678, Dec. 2014.

[4] F. Horlin, J. Fickers, P. Emplit, A. Bourdoux, and J. Louveaux, "Dual-polarization OFDM-OQAM for communications over optical fibers with coherent detection," *Opt. Express*, vol. 21, no. 5, pp. 6409–6421, 2013.

[5] Z. Li, T. Jiang, H. Li, X. Zhang, C. Li, C. Li, R. Hu, M. Luo, X. Zhang, X. Xiao *et al.*, "Experimental demonstration of 110-Gb/s unsynchronized band-multiplexed superchannel coherent optical OFDM/OQAM system," *Optics express*, vol. 21, no. 19, pp. 21 924–21 931, 2013.

[6] B. Farhang-Boroujeny, "OFDM versus filter bank multicarrier," *IEEE Signal Process. Mag.*, vol. 28, no. 3, pp. 92–112, May 2011.

[7] T. Pfau, S. Hoffmann, and R. Noe, "Hardware-Efficient Coherent Digital Receiver Concept With Feedforward Carrier Recovery for M-QAM Constellations," *Journal of Lightwave Technology*, vol. 27, no. 8, pp. 989–999, April 2009.

[8] E. Ip and J. M. Kahn, "Feedforward Carrier Recovery for Coherent Optical Communications," *Journal of Lightwave Technology*, vol. 25, no. 9, pp. 2675–2692, Sept 2007.

[9] E. Kofidis, D. Katselis, A. Rontogiannis, and S. Theodoridis, "Preamble-based channel estimation in OFDM/OQAM systems: A review ," *Signal Processing*, vol. 93, no. 7, pp. 2038 – 2054, 2013. [Online]. Available: http://www.sciencedirect.com/science/article/pii/S0165168413000169

[10] S. Randel, A. Sierra, X. Liu, S. Chandrasekhar, and P. Winzer, "Study of Multicarrier Offset-QAM for Spectrally Efficient Coherent Optical Communications," in *37th European Conference and Exposition on Optical Communications*. Optical Society of America, 2011, p. Th.11.A.1. [Online]. Available: http://www.osapublishing.org/abstract.cfm?URI=ECOC-2011-Th.11.A.1

[11] M. G. Bellanger, "Specification and design of a prototype filter for filter bank based multicarrier transmission," in *IEEE International Conference on Acoustics, Speech, and Signal Processing*, vol. 4. IEEE, 2001, pp. 2417–2420.